# Spinel $NiCo_2O_4$ and single walled carbon nanotube nanocomposites for high performance supercapacitor application

**Surjit Sahoo, Chandra Sekhar Rout***

*School of Basic Sciences, Indian Institute of Technology Bhubaneswar, Bhubaneswar 751013, India*
*Corresponding author: E-mail: csrout@iitbbs.ac.in , csrout@gmail.com

**Received: 05 December 2016, Revised: 20 December 2016 and Accepted: 23 January 2017**

DOI: 10.5185/amlett.2017.1539
www.vbripress.com/aml

## Abstract

In the present work, we report the hydrothermal synthesis of $NiCo_2O_4$/Single walled carbon nanotubes (SWNTs) nanocomposites for supercapacitor applications. The SWNTs provided the conductive network and favored the growth of $NiCo_2O_4$ nanoparticles on its surface to facilitate the collection and transportation of electrons during the electrochemical charge storage performance. Due to the improved conductivity and higher surface area of the $NiCo_2O_4$/SWNTs nanocomposites as compared to pure $NiCo_2O_4$ nanorods, it exhibited a specific capacitance of 1623 F/g and 1098 F/g at 1mV/s scan rate and 1A/g current density. Obtained energy density and power density of the $NiCo_2O_4$/SWNTs nanocomposites were 56.19 Wh/Kg and 9.824 kW/kg respectively. These results demonstrated that the nanocomposites could be a promising candidate for future high performance energy storage devices. Copyright © 2017 VBRI Press.

**Keywords:** Composites, spinel, supercapacitor, metal oxide, carbon nanotube.

## Introduction

Recently, electrochemical capacitors or widely known as supercapacitors has emerged as an alternate energy storage devices due to their high power density, fast charge/discharge rate and long cycling performance etc [**1**]. Based on the energy storage mechanisms involved in the supercapacitor performance, it has been classified as Electric double layer capacitor (EDLC) and pseudocapacitors **[2]**. Carbon based materials are known to be EDLC type whereas transition metal oxides such as $NiCo_2O_4$ **[3]**, $MnCo_2O_4$ **[4]**, $CoMoO_4$ **[5]**, $ZnCo_2O_4$ **[6]** chalcogenides such as $Ni_3S_2$ **[7]**, Ni-Co sulfide **[8]**, Mn-Co sulfide **[9]**, $CuSe_2$ **[10]** and conducting polymers **[11]** are pseudocapacitive materials **[12]**. Though pseudocapacitors deliver higher capacitance and energy density than EDLCs, they have drawbacks with low power density and cycling stability. To overcome these drawbacks, enormous effort have been put to prepare hybrid materials and asymmetric supercapacitors in which combinations of EDLC type and pseudocapacitive materials have been utilized **[13]**.

Ternary transition metal oxides and their nanocomposites have been received huge interest in recent years due to their promising enhanced electrochemical properties **[14]**. Among all the mixed transition metal oxides, the ternary metal oxides (MTMOs) with two different metal cations have received tremendous attention in many energy related application. Among different (MTMOs), $NiCo_2O_4$ belongs to the group of normal spinels and has a space symmetry group of Fd 3m. $NiCo_2O_4$ not only have attractive features including its low cost and natural abundance but also exhibits different diverse nanostructures which are feasible for superior electrochemical performance **[15]**. Similarly, among all the carbonaceous material, SWCNT is an attractive candidate for high performance electrode material of supercapacitor due to its high conductivity, low mass density, large specific surface area and high mechanical strength **[16]**. The enhanced electrochemical performance of $NiCo_2O_4$/SWNTs nanocomposites could be attributed to the synergistic effect of both nanorods shape $NiCo_2O_4$ and highly conductive SWCNTs.

$NiCo_2O_4$ is a ternary spinel transition metal oxide of such category with enhanced electronic conductivity and electrochemical properties as well as exhibits different diverse nanostructure which are beneficial for designing hybrid supercapacitor materials **[15]**. Similarly compared to other carbonaceous materials, SWNTs provide a higher electronic conductivity due to the decreased contact resistance from fewer interparticle contacts **[17]**. Recently, different morphology of $NiCo_2O_4$-nanocarbon hybrid composites have been designed for supercapacitor applications. Luo *et al.* reported supercapacitor performance of $NiCo_2O_4$-RGO hybrids with a specific capacitance of 777.1 F/g at 5A/g **[18]**. Cai *et al*. achieved a capacitance of 1038 F/g at 0.5A/g current density by selecting MWNTs as conductive support for ultra-thin $NiCo_2O_4$-nanosheets **[19]**. Li *et al.* reported fabrication of core-shell structure of carbon/$NiCo_2O_4$ sub microspheres with a specific capacitance up to 1420 F/g at 1A/g **[20]**.

 

Notably, little research works has been done based on $NiCo_2O_4$ and SWCNT composite material. On the basis of previous reports, there are several challenges to enhance the electrochemical performance as well as energy density of $NiCo_2O_4$ by adding carbonaceous conductive materials like RGO, CNT and quantum dots. Here we prepared mixed composite of $NiCo_2O_4$ nanorods and functionalized SWCNT by a facile hydrothermal approach. This novel composite material exhibits excellent supercapacitive performance with high specific capacitance of 1623 F/g. The ultrafine hybrid structure provides more contact area for improvement of its electrochemical reaction. So it has been established that the addition of carbonaceous conductive material absolutely plays crucial role for the improvement of electrochemical activity. Herein we report a facile hydrothermal method for the preparation of $NiCo_2O_4$/SWNTs nanocomposites with the aim to provide conductive network by using SWNTs. The growth of $NiCo_2O_4$ nanoparticles on SWNTs helped to fabricate the collection and transportation of electrons during the electrochemical charge storage performance to achieve electrochemical properties.

## Experimental

*Materials synthesis*

For the synthesis of $NiCo_2O_4$, Nickel nitrate hexahydrate [$Ni(NO_3)_2$. 6 $H_2O$, 98%, Merck India], Cobalt nitrate hexahydrate [$Co(NO_3)_2$. $6H_2O$, 97%, Merck India] and urea [$CH_4N_2O$, 99.5%, Sisco Research laboratories, India] were used. The SWNTs supplied by Reinste Nano ventures Private Limited (diameter: 1.1 to 1.7 nm, length: few µm) were used to prepare $NiCo_2O_4$/SWNTs nanocomposites after treating the SWNTs in $H_2SO_4$ and $HNO_3$ (3:1) mixture.

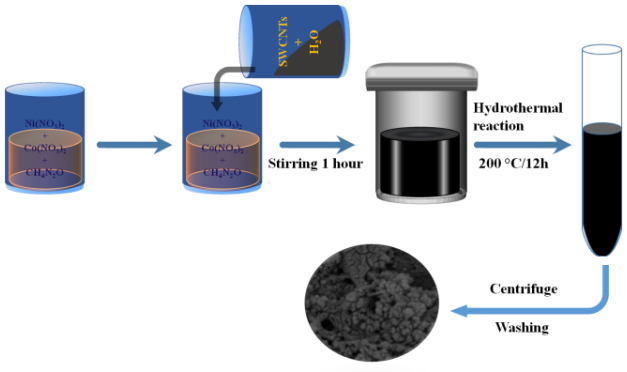


**Fig. 1.** Schematic diagram showing the synthesis processes involved for the preparation of $NiCo_2O_4$/SWNTs nanocomposites.

For the preparation of $NiCo_2O_4$/SWNTs nanocomposites 40 mg of functionalized SWNTs were dispersed in 20 ml DI water. In a separate beaker, 3 mM of Nickel nitrate hexahydrate and 6 mM Cobalt nitrate hexahydrate and 60 mM urea were dissolved in 20 ml DI water and a clear solution was achieved. Then these two solutions containing the transition metal precursors and SWNTs were added to a 50 ml Teflon-lined stain-less steel autoclave. Hydrothermal reaction was carried out at 200 °C for 12h and the obtained product was washed in ethanol and DI water. Finally, the product was dried in vacuum at 80 °C for 6h.

**Fig. 1** shows the schematic diagram of the synthesis process of $NiCo_2O_4$/SWNTs nanocomposites. Urea helps to hydrolyze the transition metal precursors. In the presence of SWNTs, the solution containing urea, nickel and cobalt ions get nucleated on the SWNTs walls to form the $NiCo_2O_4$/SWNTs nanocomposites. Also, we performed the same hydrothermal reaction in the absence of SWNTs and only $NiCo_2O_4$ nanorods were formed without SWNTs.

*Characterizations*

The samples were characterized by FESEM (MERLIN Compact with GEMINI I electron column, Zeiss Pvt. Ltd., Germany) and by elemental mapping with EDAX. X-ray diffraction (XRD) patterns of the samples were obtained by a Bruker D8 Advanced diffractometer using Cu-$K_\alpha$ radiation (wavelength =1.54184 Å).

*Evaluation of electrochemical property*

To measure the supercapacitor performance of the samples, a three-electrode electrochemical cell with a Potentiostat/Galvanostat (PG-16125, Techno Science instrument, Bangalore, India) was used. The cyclic voltammetry (CV) charge-discharge (CD) measurements were performed in 2M aqueous KOH solution and the working window was kept between -0.1 to 0.4 V vs. Ag/AgCl electrode. Glassy carbon electrode was used as the working electrode, Ag/AgCl as the reference and spiral Pt wire as the counter electrode.

The surface of the glassy carbon electrode was polished with micro-polishing powder ($Al_2O_3$ powder having grain sizes such as 1.0 µm, 0.3 µm and 0.05 µm) to achieve a mirror finish and it was subsequently sonicated with DI water for about 15 min in order to remove any adsorbed species on the electrode surface. To prepare the homogeneous mixture solution of the samples, about 1 mg of the as-synthesized sample was dispersed in an ethanol/nafion (95 µl/5µl mixture) and ultra-sonicated for 15 min. After achieving a uniform dispersion, 2.5 µl of mixture solution was drop-casted on to the freshly polished glassy carbon electrode and then it was dried in a vacuum desiccator for 1h. The mass of the deposited sample on the glassy carbon electrode was found to be 0.17 mg. The specific capacitance, energy density and power density were calculated by using the formulae and procedure as discussed in our previous reports **[21]**.

## Results and discussion

**Fig. 2a** and **b** show the FESEM images of the $NiCo_2O_4$ nanorods. In the absence of SWNTs, the $NiCo_2O_4$ nanorods are formed with diameters of 50-60 nm range and length in the 0.2-1 µm range.

With addition of 40 mg of SWNTs, the obtained $NiCo_2O_4$/SWNTs nanocomposites consist of $NiCo_2O_4$ nanoparticles in the 20-50 nm range, which is cross-linked with the SWNTs **(Fig. 2c, d)**.

 

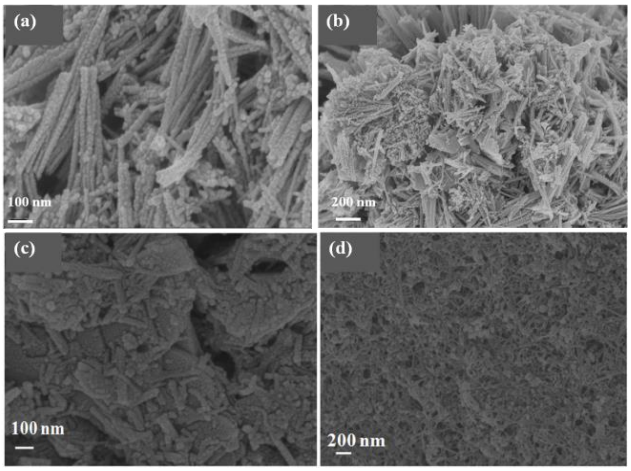


**Fig. 2.** (a) High and (b) low magnification FESEM images of $NiCo_2O_4$ nanorods. (c) High and (d) low magnification FESEM images of $NiCo_2O_4$/SWNTs nanocomposites.

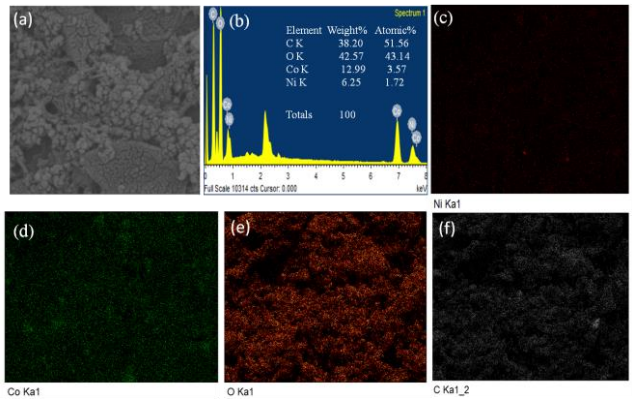


**Fig. 3**. EDAX mapping of the elements present in $NiCo_2O_4$/SWNTs nanocomposites. (a) FESEM image of the region from where mapping data has been collected. (b) EDAX spectra with inset showing elements present. Mapping of (c) Ni, (d) Co, (e) O and (f) C.

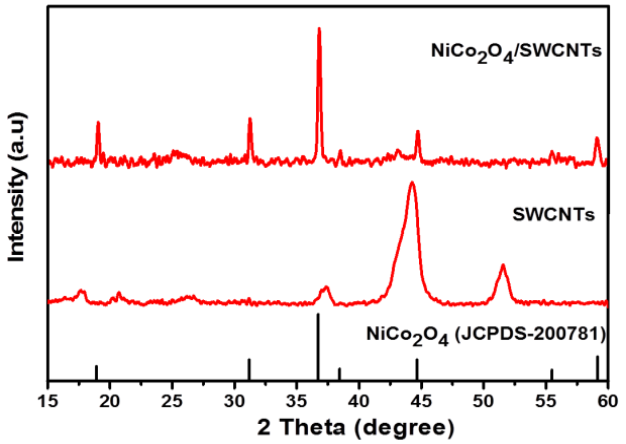


**Fig. 4**. XRD pattern of $NiCo_2O_4$/SWNTs nanocomposites and SWNTs.

The EDAX spectrum of the $NiCo_2O_4$/SWNTs nanocomposites as shown in **Fig. 3b** suggests the presence of Ni, Co, O and C with an approximate atomic ratio of Ni and Co to be 1:2 confirming the formation of $NiCo_2O_4$. The elemental mapping of the sample is shown in **Fig. 3** and it confirms the uniform distribution of the elements in the sample. **Fig. 4** shows the XRD pattern of the $NiCo_2O_4$/SWNTs nanocomposites and SWNTs. The extra peaks observed in the case of SWNTs sample are due to the catalyst used for the preparation of the nanotubes. The XRD pattern of the $NiCo_2O_4$/SWNTs nanocomposites match with the JCPDS no: 20-0781 and it can be assigned to face centered cubic crystal of spinel $NiCo_2O_4$. The peaks of $NiCo_2O_4$ dominated the SWNTs due to low content of the CNTs in the sample. The formation process of $NiCo_2O_4$/SWNTs nanocomposites can be explained as follows. Ni and Co ions in the presence of urea get adsorbed on the surface of SWNTs since the CNTs are known to be a common metal ion adsorbent **[19]**. Also, the metal ions prefer to attach at the defect sites of the CNTs surface and the defect sites act as heterogeneous nucleation sites in the early reaction stage to facilitate the formation of $NiCo_2O_4$ crystals. At further stage, the small crystals formed get aggregated to form $NiCo_2O_4$ nanoparticles.

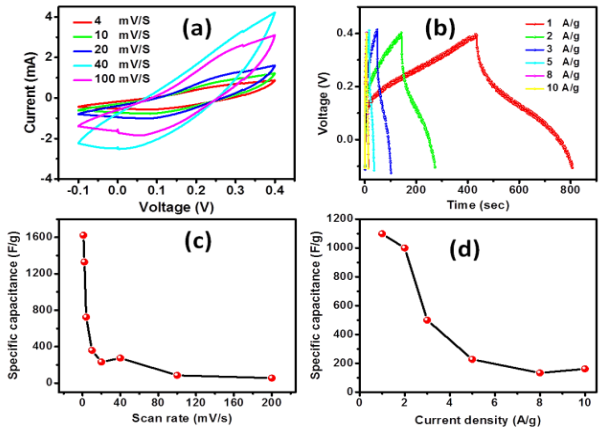


**Fig. 5**. Electrochemical supercapacitor performance of $NiCo_2O_4$/SWNTs nanocomposites: (a) CVs at different scan rates, (b) CDs at different discharge current, variation in specific capacitance at different (c) scan rates and (d) discharge currents respectively.

The electrochemical performance of the $NiCo_2O_4$/SWNTs nanocomposites were investigated by CV and galvanostatic CD techniques in 2M KOH. **Fig. 5a** shows the CV curves with various scanning rates ranging from 4 to 100 mV/s. In CVs, the shifting of redox peaks occur due to the internal resistance of electrode and polarization phenomenon involved due to the faster electron transfer process at high scan rates on the surface electrode material **[22]**. The intimate binding of $NiCo_2O_4$ and SWNTs affords facile electron transport between individual $NiCo_2O_4$ and SWNT which lead to achieve enhanced charge storage performance as compared to bare SWNTs and $NiCo_2O_4$. The possible redox mechanisms in the KOH electrolyte are based on the following equations: **[23]**

$$NiCo_2O_4 + OH^- + H_2O \leftrightarrow NiOOH + 2CoOOH + 2e^-$$

$$CoOOH + OH^- \leftrightarrow CoO_2 + H_2O + e^-$$

A comparative supercapacitor performance of SWNTs, $NiCo_2O_4$ and $NiCo_2O_4$/SWNTs nanocomposites are shown in **Table 1**. The galvanostatic discharge curves between -

 

0.1 and 0.4 V at different specific currents are shown in **Fig. 5b**. The nanocomposites exhibited the specific capacitance of 1623, 1333, 750 and 400 F/g at a scan rate of 1, 2, 5 and 10 mV/s respectively which are much higher than the pure $NiCo_2O_4$ nanorods as reported by us in our previous work **[21]**. The CD curves of $NiCo_2O_4$/SWNTs shows the pseudocapacitive character of material, in which discharge curve consist of two section. In discharge curve a rapid potential drop occurs due to the internal resistance and a sluggish potential drop originating from redox reaction **[24]**. The obtained specific capacitance values were 1098 F/g at 1A/g current density which is shown in **Fig. 5d**.

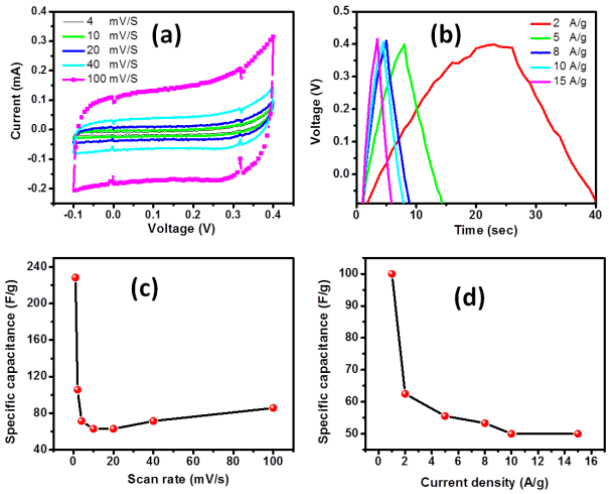


**Fig. 6**. Electrochemical supercapacitor performance of bare SWNTs: (a) CVs at different scan rates, (b) CDs at different discharge current, variation in specific capacitance at different (c) scan rates and (d) discharge currents respectively.

The CVs, CDs and variation of specific capacitance with respect to scan rate and discharge current for the SWNTs are shown in **Fig. 6.** A highest specific capacitance of 230 F/g at 1mV/s scan rate and 100 F/g at a current density of 1A/g was obtained for the SWNTs. Obtained energy density were **6.9, 28.5** and **56.19 Wh/kg** for SWNTs, $NiCo_2O_4$ and $NiCo_2O_4$/SWNTs nanocomposites respectively. Similarly, the calculated power densities were 3.119, 4.438 and 9.824 kW/kg for SWNTs, $NiCo_2O_4$ and $NiCo_2O_4$/SWNTs nanocomposites respectively. The intimate binding of $NiCo_2O_4$ and SWNTs affords facile electron transport could be ascribed to the highest conductivity of SWCNT and interconnected nanoparticles of $NiCo_2O_4$ and it enhances the flexibility and conductivity of the $NiCo_2O_4$/SWCNTs electrode material, supplying shortened electron and ion transport pathways during charging and discharging [**25**]. The $NiCo_2O_4$ strongly anchored on the SWCNTs surface to form a peculiar structure with outstanding stability and integrity [**23**]. The ultrafine structures provide largest contact area and favor the faster transportation of $OH^-$ ions by significantly lessening its diffusion length and increasing the accessible sites [26]. From the above analysis, it is clearly observed that the $NiCo_2O_4$/SWNTs nanocomposites show enhanced supercapacitor performance as compared to the bare SWNTs and $NiCo_2O_4$ nanorods as well as previous reported results **(Table 2)**.

**Table 1.** Comparison of the supercapacitor performance of $NiCo_2O_4$, SWNTs and $NiCo_2O_4$/SWNTs nanocomposite.

| Sample | Specific capacitance (F/g) | Energy-density (Wh/Kg) | Power-density (kW/kg) |
|---|---|---|---|
| SWCNTs | 200 | 6.925 | 3.119 |
| $NiCo_2O_4$ | 823.52 | 28.51 | 4.438 |
| $NiCo_2O_4$-SWCNTs | 1623 | 56.19 | 9.824 |

**Table 2.** Summary of electrochemical supercapacitor performance of $NiCo_2O_4$, SWCNT and their hybrid composites.

| Material | Preparation method | Specific Capacitance (F/g) | Ref |
|---|---|---|---|
| $NiCo_2O_4$ | Hydrothermal | 658 | [**27**] |
| $NiCo_2O_4$ | Hydrothermal | 372 | [**28**] |
| $NiCo_2O_4$ | Chemical bath deposition | 490 | [**29**] |
| $NiCo_2O_4$ | Solution method | 401 | [**30**] |
| $NiCo_2O_4$ | Sol-gel | 217 | [**31**] |
| SWCNT | CVD | 178 | [**32**] |
| SWCNT | - | 35 | [**16**] |
| $NiCo_2O_4$-SWCNT/Ni Foam | Hydrolysis | 1642 | [**23**] |
| $NiCo_2O_4$- CNT | CVD | 828 | [**25**] |
| SWCNT - (Functionalized) | - | 200 | This Work |
| $NiCo_2O_4$-SWCNT/GC electrode | Hydrothermal | 1623 | This Work |

## Conclusion

In summary, the $NiCo_2O_4$/SWNTs nanocomposites were synthesized by a facile hydrothermal method. The defects in the SWNTs played an important role for the formation of $NiCo_2O_4$ nanoparticles whereas $NiCo_2O_4$ nanorods were formed without SWNTs under the same hydrothermal condition. The improved conductivity and high surface area of the nanocomposites lead to better supercapacitor performance as compared to bare $NiCo_2O_4$ and SWNTs. The $NiCo_2O_4$/SWNTs nanocomposites exhibited a specific capacitance of 1632 F/g and 1100 F/g at 1mV/s scan rate and 1A/g current density respectively. The enhanced electrochemical supercapacitor performance of the $NiCo_2O_4$/SWNTs demonstrates its capability for the next generation energy storage device.

#### Acknowledgements

Dr. C.S. Rout would like to thank DST (Government of India) for the Ramanujan fellowship (Grant No. SR/S2/RJN-21/2012). This work was supported by the DST-SERB Fast-track Young scientist (Grant No. SB/FTP/PS-065/2013), UGC-UKIERI thematic awards (Grant No. UGC-2013-14/005) and BRNS-DAE, (Grant

 

No. 37(3)/14/48/2014-BRNS/1502). Also, part of this work is supported by the Indo-US Science and Technology Forum (IUSSTF) through a joint INDO-US centre grant and Ministry of Human Resources Development (MHRD), India through a center of excellence grant.

**References**


1. Chee, W.K.; H. N. Lim, H.N.; Zainal, Z.; Huang, N.M.; I. Harrison, I.; Andou, Y. *J. Phys. Chem. C*, **2016**, 120 , 4153. **DOI:** 10.1021/acs.jpcc.5b10187
2. Wu, J.B.; Guo, R.Q.; Huang, X.H.; Lin, Y. *J. of Power Sources*, **2013**, 243, 317. **DOI:** 10.1016/j.jpowsour.2013.05.165
3. Sahoo, S.; Ratha S.; Rout, C.S. *Am. J. of Eng. and Appl. Sci.*, **2015**, 8, 371. **DOI:** 10.3844/ajeassp.2015.371.379
4. Sahoo, S.; Naik, K.K.; Rout, C.S. *Nanotechnology*, **2015**, 26, 455401. **DOI:** 10.1088/0957-4484/26/45/455401
5. Veerasubramania, G.K.; Krishnamoorthy, K.; Kim, S.J. *J. of Power Sources*, **2016**, 306, 378. **DOI:** 10.1016/j.jpowsour.2015.12.034
6. Karthikeyan, K.; Kalpana, D.; Renganathan, N.G. *Ionics* **2009**, 15, 107 **DOI:** 10.1007/s11581-008-0227-y
7. Krishnamoorthy, K.; Veerasubramani, G.K.; Radhakrishnana, S.; Kim, S.J. *Chem. Eng. J.* **2014**, 251, 116. **DOI:** 10.1016/j.cej.2014.04.006
8. Sahoo, S.; Naik, K.K.; Late, D.J.; CS Rout, C.S. *J. of Alloys and Compounds*, **2017**, 695, 154. **DOI:** 10.1016/j.jallcom.2016.10.163
9. Sahoo, S.; CS Rout, C.S. *Electrochimica Acta*, **2016**, 220, 57. **DOI:** 10.1016/j.electacta.2016.10.043
10. Pazhamalai, P.; Krishnamoorthy, K.; Kim, S.J. *Int. J. of Hydrogen Energy*, **2016**, 41, 1483. **DOI:** 10.1016/j.ijhydene.2016.05.157
11. Snook, G.A.; Kao, P.; Best. *A.S.; J. of Power Sources*, **2011**, 196, 1 DOI: 10.1016/j.jiec.2016.01.031
12. Li, X.; Sun,W.; Wang, L.; Qi, Y.; Guo, T.; Zhao,X.; Yan, X. *RSC Adv.*, **2015**, 5, 7976. **DOI:** 10.1039/C4RA09048A
13. Pendashteh, A.; Rahmanifar, M.S.; Kaner, R.B.; Mousavi, M.F. *Chem. Commun.*, **2014**, 50, 1972. **DOI:** 10.1039/C3CC48773C
14. Dubal, D.P.; O. Ayyad, O.; V. Ruiza, V.; Romero, P.G. *Chem. Soc. Rev.*, **2015**, 44, 1777. **DOI:** 10.1039/C4CS00266K
15. Dubal, D.P.; Romero, P.G.; Sankapal, B.R.; Holze, R. *Nano Energy*, **2015**, 11, 377. **DOI:** 10.1016/j.nanoen.2014.11.013
16. Niu, Z.; Zhou, W.; Chen, J.; Feng, G.; Li, H.; Ma, W.; Jinzhu Li, J.; Dong, H.; Ren, Y.; Zhao, D.; Xie S.; *Energy Environ. Sci.*, **2011**, 4, 1440 **DOI:** 10.1039/C0EE00261E
17. Kaempgen, M.; Chan, C.K.; Ma, J.; Cui, Y.; Gruner, G. *Nano Lett.*, **2009**, 9, 1872. **DOI:** 10.1021/nl8038579
18. Luo, Y.; Zhang, H.; Guo, D.; Ma, J.; Li, Q.; Chen, L.; Wang, T. Electrochim. Acta, **2014**, 132, 332. **DOI:** 10.1016/j.electacta.2014.03.179
19. Cai, F.; Kang, Y.; Chen, H.; Chen, M.; Li, Q. *J. Mater. Chem. A*, **2014**, 2, 11509. **DOI:** 10.1039/C4TA01235F
20. Li, D.; Gong, Y.; Zhang, Y.; Luo, C.; Li, W.; Fu, Q.; Pan, C. *Sci. Reports*, **2015**, 5, 12903. **DOI:** 10.1038/srep12903
21. Sahoo, S.; Ratha S.; Rout, C.S. *Am. J. of Engineering and Appl. Sci.*, **2015**, 8, 371. **DOI:** 10.3844/ajeassp.2015.371.379
22. Yang, D.; Ge, F.; Tian, M.; Ning, N.; Zhang, L.; Zhao, C.; Ito, K.; Nishi, T.; Wang, H.; Luan, Y. *J. Mater. Chem. A*, **2015**,3, 9468. **DOI:** 10.1039/C5TA01182E
23. Wang, X.; Han, X.; Lim, M.; Singh, N.; Gan, C.L.; Jan, M.; Lee, P.S. *J. Phys. Chem. C*, **2012**, 116, 12448. **DOI:** 10.1021/jp3028353
24. Mei, L.; Yang, T.; Xu, C.; Zhang, M.; Chen, L.; Li, Q.; Wang, T. *Nano Energy*, **2014**, 3, 36. **DOI:** 10.1016/j.nanoen.2013.10.004
25. Li, J.; Qu, J.; Yang, R.; Qu, L.; de B Harrington P.; *Electroanalysis*, **2016**, 28, 1 **DOI:** 10.1002/elan.201500490
26. Peng, T.; Yi, H.; Sun, P.; Jing, Y.; Wang, R.; Wang, H.; Wang X.; *J. Mater. Chem. A*, **2016**, 4, 8888 **DOI:** 10.1039/C6TA02410F
27. Qi Lu, Q.; Yunpeng Chen, Y.; Wanfeng Li, W.; Chen, G.; Xiao, Q.; Jiao, F.; *J. Mater. Chem. A*, **2013**,1, 2331 **DOI:** 10.1039/C2TA00921H
28. Kuang, M.; Zhang, W.; Guo, X.L.; Yu, L.; Zhang Y.X.; *Ceram. Int.* **2014**, 40, 10005 **DOI:** 10.1016/j.ceramint.2014.02.099
29. Salunkhe, R.R.; Jang, K.; Yu, H.; Yu, S.; Ganesh, T.; Han, S.-H.; Ahn H.; *J. Alloys Compd.* **2011**, 509, 6677 **DOI:** 10.1016/j.jallcom.2011.03.136
30. Xiao, J.; Yang , *S.; RSC Adv.*, **2011**,1, 588 **DOI:** 10.1039/C1RA00342A
31. Wu, Y.Q.; Chen, X.Y.; Ji, P.T.; Zhou Q.Q.; *Electrochim. Acta* **2011**, 56, 7517 **DOI:** 10.1016/j.electacta.2011.06.101
32. Kanninen, P.; Luong, N.D.; Sinh, L.H.; Anoshkin, I.V.; Tsapenko, A.; Seppälä, J.; Nasibulin,A.G.; Kallio, T.; *Nanotechnology* **2016** 27, 235403 **DOI:** 10.1088/0957-4484/27/23/235403


 